1-1-2007

Analysis of particle motion in a micro-fluidic dielectrophoretic device

Weihua Li
University of Wollongong, weihuali@uow.edu.au

X Z. Zhang
University of Wollongong

Analysis of Particle Motion in a Micro-Fluidic Dielectrophoretic Device

W.H. Li, and X. Z. Zhang

School of Mechanical, Materials and Mechatronic Engineering, University of Wollongong,
Northfields Avenue, NSW 2522, Australia

Abstract: - Interdigitated microelectrodes have found wide applications in manipulating and/or separating biological particles due to their simple structure and easy implementation. Particle behaviors in such interdigitated microelectrode devices are affected by a number of factors, including particle size, electrical potential, chamber geometry and dielectric properties. This paper presents systematical simulation study of particle behaviors in these devices by considering all these influencing factors. A case study is presented to separate different particles using both positive and negative DEP.

Key-Words: - Dielectrophoresis, interdigitated microelectrodes, DEP forces, hydrodynamic drag force, buoyancy force, particle motion

1 Introduction

Recent study in lab-on-a-chip shows a growing interest in exploiting the use of dielectrophoresis (DEP) to manipulate or separate bioparticles, such as cells, bacteria, viruses and DNA [1]. DEP is the physical phenomenon that a particle moves towards the regions of high field intensity (positive DEP) or low field intensity (negative DEP) when exposed to non-uniform electric fields. The mechanism of DEP arises from the polarization of particles and non-uniform forces exerted by external fields [2]. The DEP force depends on the arrangement of the electrode and the resulting electric field distribution as well as dielectric properties of the particle and the surrounding medium, this leads to several possible electrode arrange design configurations that can be used to manipulate and separate particles, including interdigitated electrode arrays [3,4], polynomial design [5], castellated design [6], and cage design [7]. Among these electrode configurations abovementioned, the interdigitated electrode array is widely used to separate or manipulate bioparticles. In this case, the DEP force is generated using an array of interdigitated planar electrodes that form the bottom of a flow-through chamber. By considering the coupling of the DEP force, the hydrodynamic force and the sedimentation force, the particles with different properties will be levitated to different heights (negative DEP) or be trapped along the electrode edges [3].

This paper presents a dynamic study to investigate biopartilce motion in a typical interdigitated micro-fluidic device. The effects of several important factors, including particle size, initial height and electric field on the particle behavior is addressed. These simulation results on the issues of design and optimization of DEP devices are also discussed.

2 Theoretical Background

2.1 Schematic of Interdigitated Electrodes

The schematic of the interdigitated microfluidic device is shown in Fig. 1a. The width of electrode stripe is d_1 and the spacing between adjacent electrodes is d_2. The configuration exhibits periodicity with period defined by $d=(d_1+d_2)/2$. Voltages V_0 and $-V_0$ are applied to adjacent electrode pairs. Since the electrodes are quite long compared to their width, the problem can be simplified as two-dimensional, as shown in Fig. 1b. The potential distribution is calculated by solving the Laplace equation in a solution cell [8], as shown in Fig. 1b.
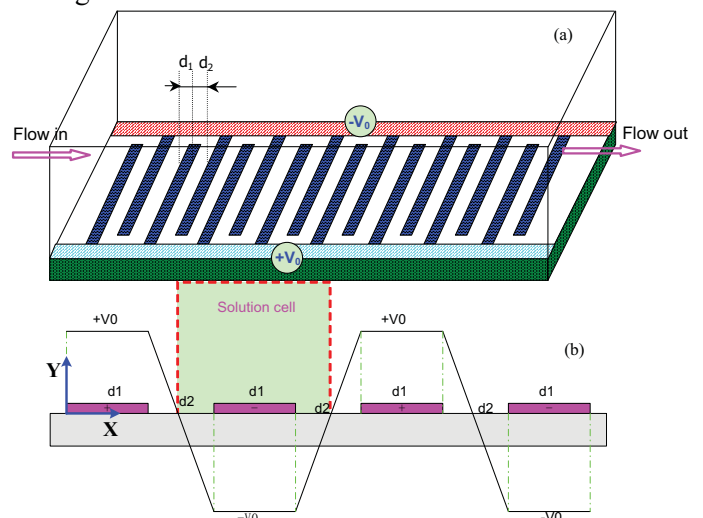

Fig. 1. (a) Schematic of the interdigitated microfludic dvices; (b) 2-D boundary condition and solution cell.

2.2 Simulation Results
Particles in the microfludic device are subjected to three kinds of forces: DEP forces, hydrodynamic drags, and sedimentation forces.

2.2.1 DEP forces
For an isotropic, homogeneous dielectric spherical particle, the time-averaged DEP force is given by

$$F = 2\pi\varepsilon_0\varepsilon_m r^3 \, \text{Re}[f_{CM}]\nabla|E_{rms}|^2 \qquad (1)$$

where $\varepsilon_0 = 8.854\times10^{-12} Fm^{-1}$ is the permittivity of free space, ε_m is the relative permittivity of the surrounding medium, r is the particle radius, E_{rms} is the root mean square value of the electric field, and f_{CM} is the Clausius-Mossotti factor, which is a complex function of the medium and particle complex permittivities [2]

$$f_{CM} = \frac{\varepsilon_p^* - \varepsilon_m^*}{\varepsilon_p^* + 2\varepsilon_m^*} \qquad (2)$$

where ε_p^* and ε_m^* are the complex permittivity of the particle and the suspending medium, defined by $\varepsilon^*=\varepsilon\text{-j}(\sigma/\omega)$ with ε as permittivity, σ conductivity and j as square root from -1. This factor can be positive or negative depending on the frequency and is therefore responsible for positive or negative DEP. For the solution cell, the numerical expressions of DEP forces in terms of x component and y component are

$$\left(F_{DEP}\right)_x = 2\pi\varepsilon_m r^3 \, \text{Re}[f_{CM}]\cdot\left(E_x E_{x,x} + E_y E_{y,x}\right) \qquad (3)$$

$$\left(F_{DEP}\right)_y = 2\pi\varepsilon_m r^3 \, \text{Re}[f_{CM}]\cdot\left(E_x E_{x,y} + E_y E_{y,y}\right) \qquad (4)$$

where E_x, E_y are x and y components of the electric field, and $E_{x,x}$, $E_{x,y}$, $E_{y,x}$, $E_{y,y}$ are gradients of electric field components.

Fig. 2 shows x component of DEP forces at different heights. As can been seen from this figure, the forces starts at zero and increases sharply to a maximum value at the edge of the electrode. Then, the DEP force suddenly drops to a negative minimum value which is very close to the electrode edge. Then the DEP force increase steadily to zero at the center of the electrode. The force distribution at the right half solution cell is anti-symmetric to the left half along the x-axis. It should be noted that the maximum force applied to the particles are at the edge of electrode. This is because that the electric field has the maximum gradient at the edge of electrodes.

The y-component of DEP forces is shown in Fig. 3. Similar to the x component, the y-component of DEP forces has the maximum values at electrode edges while it has the minimum value at the center of electrode as well as the centre of electrode pairs.

It is noted that the y-component has no negative values. It is symmetric along the vertical line passing through the electrode centre. Also, the y-component force shows a decreasing trend with the height.
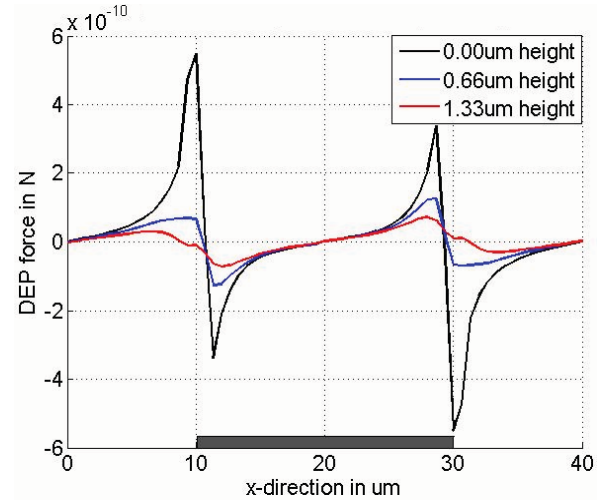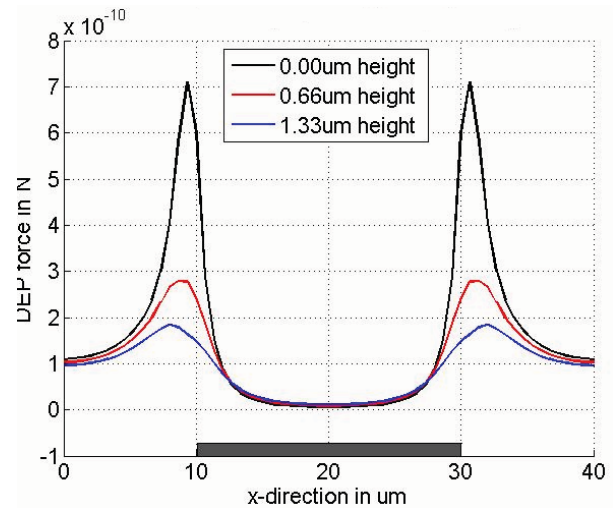

Fig. 2. x component of DEP forces at different heights.

Fig. 3. y component of DEP forces at different heights.

2.2.2 Hydrodynamic drag force
The hydrodynamic drag force on a particle of radius r is given by the modified Stokes equation [9]

$$\vec{F}_{HD-drag} = 6\pi k r\eta\left(\vec{v}_m - \vec{v}_p\right) \qquad (5)$$

where η is the dynamic viscosity of the fluid, $\vec{v}_p$ and $\vec{v}_m$ are the velocity vectors of the particle and the medium fluid at the center of the particle, k is a non-dimensional factor accounting for the wall effects. Normally, the value of k is greater than one. For a particle in contact with the wall, k is approximately equal to 1.7. The fluid is usually assumed to follow a parabolic laminar flow profile such that the velocity v at a distance y form the bottom of the chamber is:

$$v = 6\frac{\overline{V}}{wh}\frac{y}{h}\left(1 - \frac{y}{h}\right) \qquad (6)$$

where $\overline{V}$ is the nominal flow rate in μl/min, w and h are the chamber width and height respectively.

2.2.3 Hydrodynamic drag force
The sedimentation force is given by

$$F_{sedi} = \frac{4}{3}\pi r^3 \left(\rho_m - \rho_p\right)g \qquad (7)$$

where ρ_p and ρ_m are the densities of the particle and medium respectively, and g is the gravitational constant.

2.2.4 Particle motion equation
By taking into account all forces discussed above, the ordinary differential equations in terms of x and y components are obtained by using Newton's second law

$$m\ddot{x}(t) = F_{DEP,x} + 6\pi kr\left(\overline{V}_m(y) - \dot{x}(t)\right) \qquad (8)$$

$$m\ddot{y}(t) = F_{DEP,y} - 6\pi kr\,\dot{y}(t) - \frac{4}{3}\pi r^3\left(\rho_p - \rho_m\right)g \qquad (9)$$

where $x(t)$ and $y(t)$ are particle positions in x and y direction. They can be obtained by numerically solving these two equations with initial conditions of the particle position and velocity when entering the chamber. It is noted that the DEP$_x$ and DEP$_y$ are functions of position (x,y) and are obtained by linear interpolation from the calculated data and the grid points. It is assumed that the particle velocity in y direction is zero after the particle collides with the chamber bottom or top, i.e $v_y = 0|_{y=0\ or\ h}$. Friction between particle and chamber is neglected.

3 Results and Discussion
The real part of the Clausius-Mossotti factor, f_{CM}, varies from -0.5 to 1 [10]. For the simplicity, the values is set as -0.5 for negative DEP and 0.5 for positive DEP. Other parameters are listed in Table 1.

Table 1. Parameters for simulation.

ε$_m$ F/m	ε$_p$ F/m	Flow rate μl/min	ρ$_m$ g/cm^3	ρ$_p$ g/cm^3	η Pas
7.08×10^{-10}	2.21×10^{-10}	0.1	1	1.05	0.89

3.1 Negative DEP
3.1.1 Particle size effect
Suppose particles with different radii are injected to the chamber initially at the same height and the same initial conditions, as shown in Fig. 4. It can be seen that all particles reach the same levitation height about 38 μm, which implies that the final levitation position is independent of particle size but depends on physical and dielectric properties of

particle and medium. The times to reach the same levitation height for these particles were examined and shown in Fig. 5. As can been seen from this figure, the particle with larger size reaches the levitation position much quicker than those small sizes. This is because the DEP force is proportional to cubic of particle size.
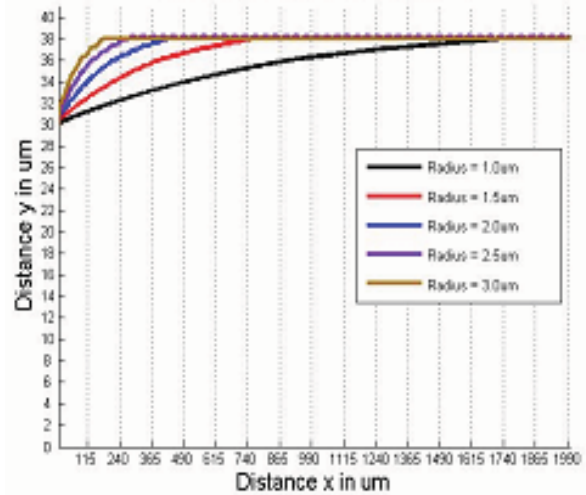

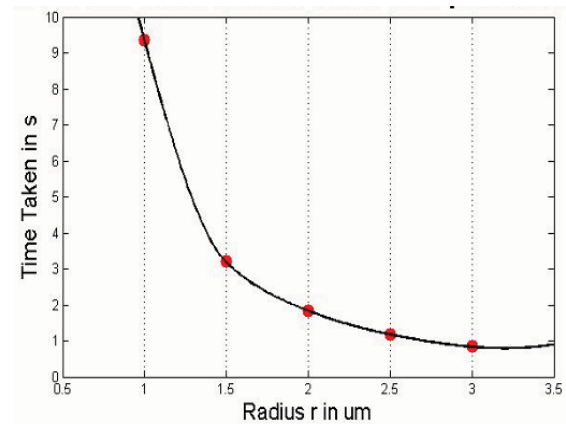Fig. 4. Particle path of different size particles under negative DEP.

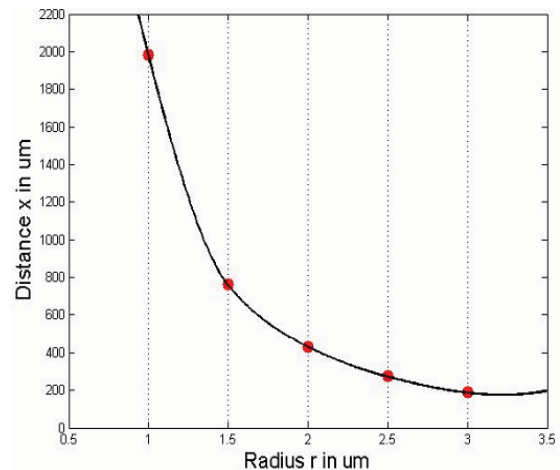Fig. 5. Time reaching levitation height vs. particle size.

Fig. 6. Taveling distance vs. particle size.

The distance in x direction when the particle reaches the levitation position versus particle size is shown in Fig. 6. As can be seen from this figure, the smallest particle, 1μm in diameter, needs a longest distance along the x-axis to levitate stably. If the device is designed to manipulate 1μm particles, the electrode array needs at least 2000μm in length for separating these particles. On the contrary, the largest particle, 3μm, only needs approximately 200μm to reach the stable stage. This result accords with the time to reach levitation as shown in Fig. 5.

3.1.2 Initial height effect

Figure 7 shows paths of all particles with the same size of 1.5μm are injected into the chamber with different initial height. As the particles have the same property constants, the particles are eventually levitated at the same approximate 38μm height in the chamber. The lowest initial height (black solid line) for a particle gives the steepest curve, whereas the highest initial height (green solid line) of a particle seems to show a linear rate of increase up to the point of particle levitation. The differences in the particle movement relate to the speed and the distance to reach stable stage points. The times and the distances for particles to reach the stable levitation stage at various initial heights are shown in Fig. 8 a and b respectively. As can be seen from these figure, the particles with smaller initial heights need take more time travel more distances than those particles with larger initial heights. For examples, the particle with the lowest initial height, 14μm, needs about 3.1s and travel 950 μm to reach the stable stage; while the particle with the highest initial height, 34μm, only needs 1.7s and travels 350 μm to levitate stably.
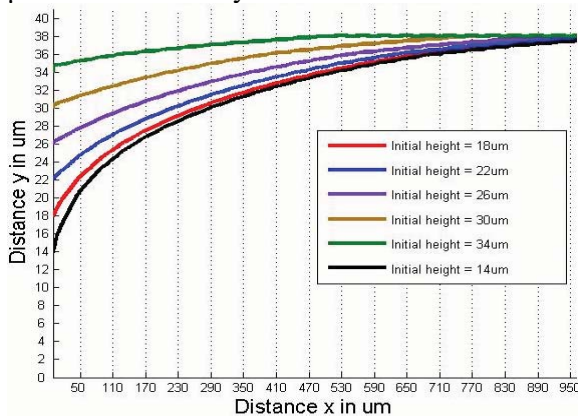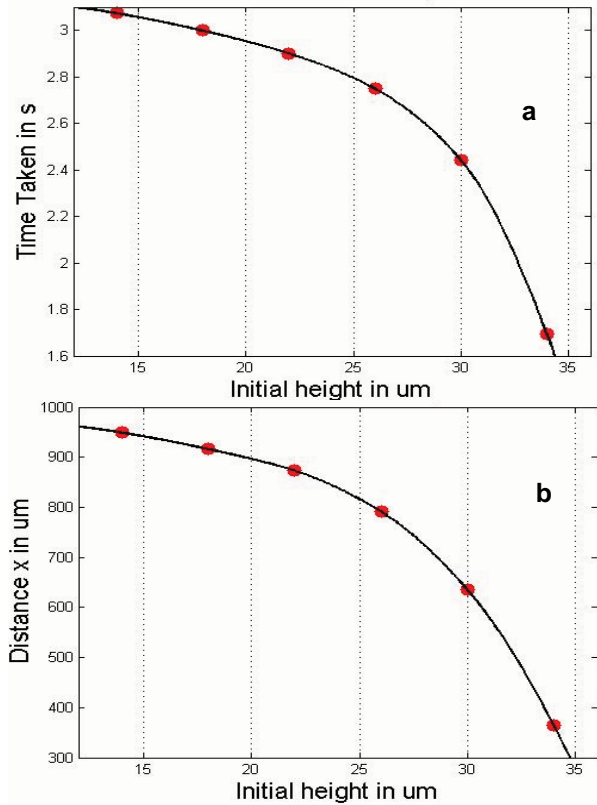

Fig. 7. Particle path with various initial heights

Fig. 8. (a) Time to reach levitation position versus initial height; (b) distance in x-axis versus initial height.

3.2 Positive DEP
3.2.1 Particle size effect

Suppose the Clausius-Mossoti value is 0.5, the particles with different particle sizes are injected into the chamber, initially at the 30μm height. The particle path is shown in Fig. 9. It can be seen from this figure that the largest particle (brown solid line) gives a sharp curved line whereas the smallest particle (black solid line) makes a gently curved line as it is trapped. All particles are all trapped at electrode edges as these areas have largest field strength changes. The stopping distance and the traveling times before being trapped are shown in Fig. 10 a and b. The smallest particle, 1μm in diameter, needs the longest time, about 1.2s, and the longest traveling distance of 660 μm for trapping. However, the largest particle, 3μm in diameter, only needs about 0.2s and travel 60 μm to reach the trapping stage. These results demonstrate that the simple device can be used to trap particles with different particle sizes.
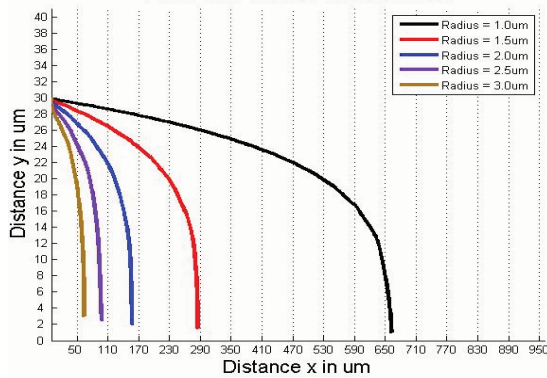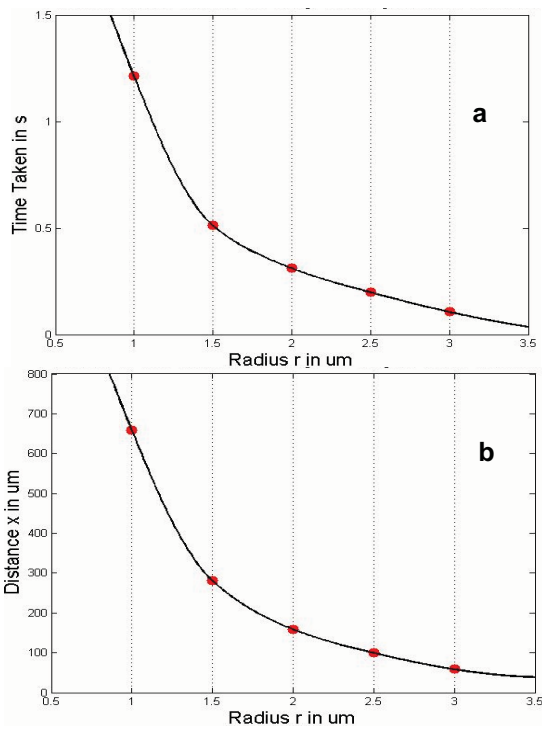
Fig. 9. Particle path for different particle sizes.

Fig. 11. Particle path with different initial heights.

Fig. 10. (a) Time to reach trapping position versus particle size; (b) traveling distance versus size.
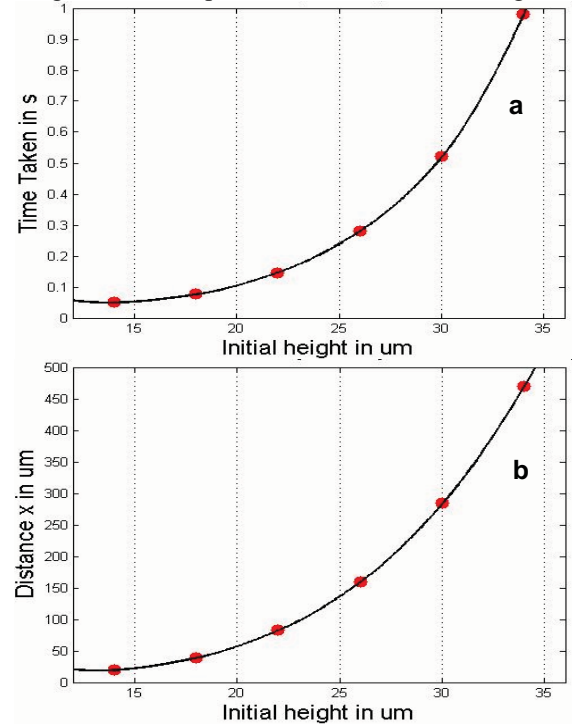
Fig. 12. (a) Travelling time vs. initial height; (b) traveling distance vs. initial height.

3.2.2 Initial height effect

For positive DEP, the effect of the initial height on the particle trapping is shown in Fig. 11. All particle have the same size but are projected into the chamber from different initial heights ranging from 14 μm to 34 μm. The higher the initial height, the longer the traveling distance. This implies the trapping position could be controlled by choosing different initial heights. The traveling time and distance before being trapped at the electrode edges are collected and shown in Fig. 12 a and b. It can be seen from these figures that both traveling time and distance show increasing trends with initial height. These results demonstrate that the initial height plays an important role in trapping particles.
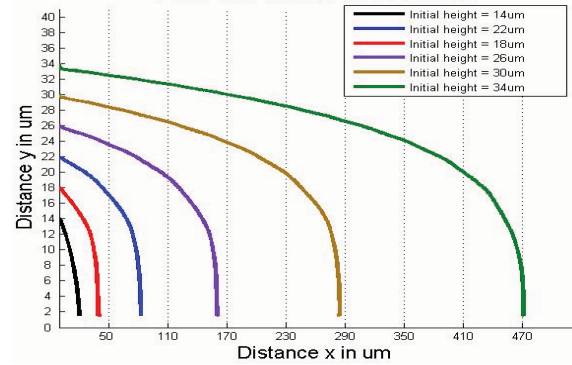
3.2.3 Voltage effect

The effect of voltage on the device trapping capacities is studied by injecting the same size particles at the same initial height but with different voltages, as shown in Fig. 13. As can be seen from this figure, the higher the voltage applied to the electrodes, the smaller traveling distance before the particle is trapped. This is obvious as the DEP force increases with electric fields. Compared with other two influencing factors, the voltage would be most effective as it is very convenient without need to change device structure. However, the voltage cannot be increased infinitely as the very high electric field would damage biological particles. To further examine the voltage effect, the relationships between the traveling time and distance versus the voltage are shown in Fig. 14 a and b.
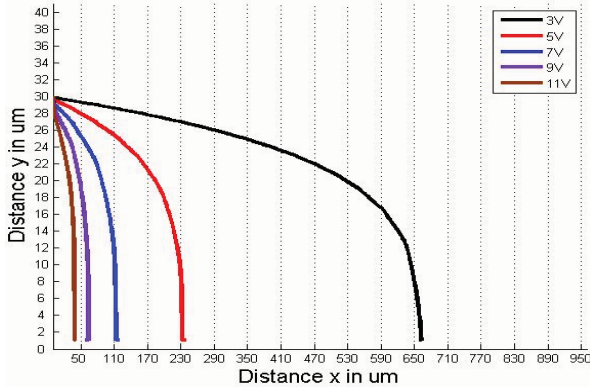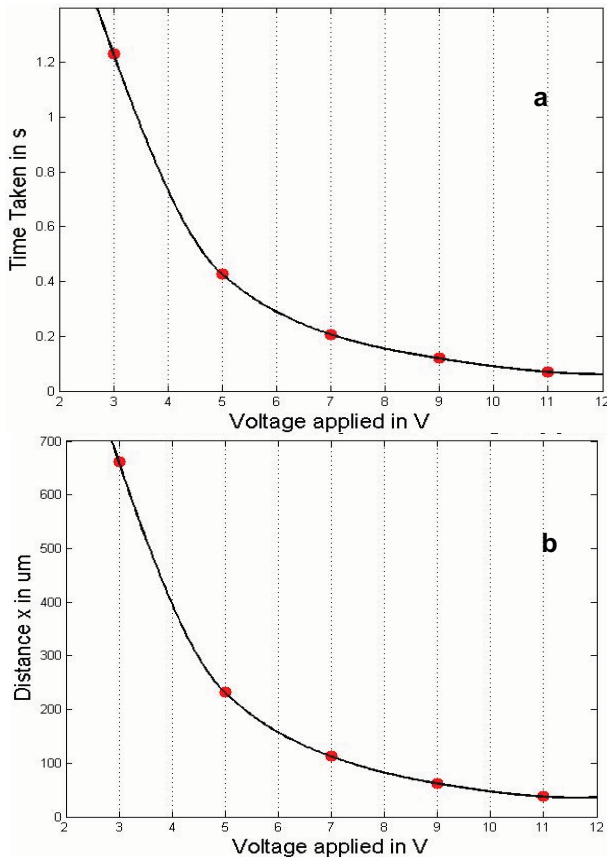
Fig. 13. Particle path at various voltages.

Fig. 14. (a) Traveling time vs. voltage; (b) traveling distance vs. voltage.

3.3 Case study

Sections 3.2 and 3.3 addressed numerical studies of negative and positive DEP by using the Clausius-Mossoti factor as -0.5 and 0.5 respectively. In practice, the factor is not always a constant as it depends on the dielectric constants of particles and medium as well as the driving frequency [2]. This case study aims to manipulate or separate a complex system consisting of two kinds of particles. Table 2 shows the particle properties of the three particles.

Table 2. Particle properties.

Particles	Density g/cm^3	Dielectric constant F/m
Latex	1.05	2.21×10^{-11}
Silicon	2.33	1.03×10^{-10}
Titanium dioxide	4.23	8.85×10^{-10}

From equation (2), the real part of the Clausius-Mossotti factor can be obtained and listed in Table 3.

Table 3. Real part of Clausias-Mossotti factor.

Particles	Re[f$_{CM}$]
Latex	-0.48
Silicon	-0.40
Titanium dioxide	0.077

A 3V voltage is applied to the system, and the mixed particles are injected at 20 μm initial height and at the centre of the chamber. The particle motions are calculated and shown in Fig. 15. As can be seen from this figure, the titanium dioxide particle is trapped in the electrode edge around 110 μm distance in x direction due to positive DEP; while the latex and silicon particles are levitated at different heights.
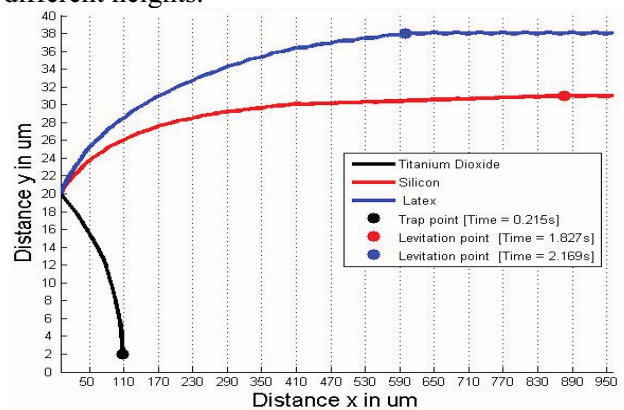

Fig. 15. Particle path for three types of particles.

However, the separation of latex and silicon would be difficult as both these two particles are levitated close to each other in the top half (>20 μm) in the chamber. The levitating particles would follow the flow stream and both types of particles would be collected at outlet 1, as shown in Fig. 16. One option to separate them is to decrease rate of outlet 2. In this case, the levitation heights of latex and silicon are 38 μm and 31 μm respectively. The required flow rate of outlet 2 can be calculated by the following equation

$$\frac{H_{silicon}}{H_{chamber}}Q_{inlet} < Q_{inlet2} < \frac{H_{latex}}{H_{chamber}}Q_{inlet} \qquad (10)$$

where $H_{silicon}$ and H_{latex} are the levitation height of the silicon and latex. $H_{champer}$ is the chamber height of the system, and Q represents the flow rate. Substitute parameters into Equation (10), the flow rate for outlet 2 should be in the range between 0.775 and 0.95 of the inlet flow rate in order to separate these two particles successfully, as shown in Fig. 17.
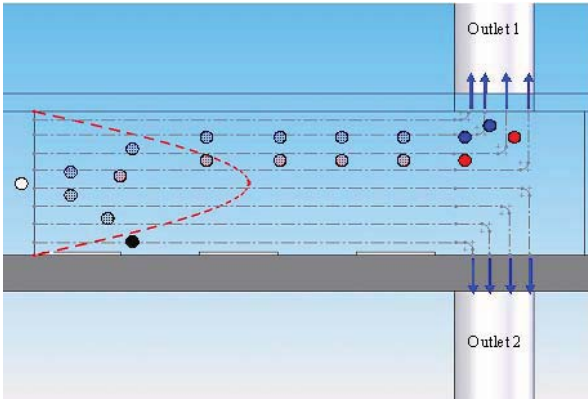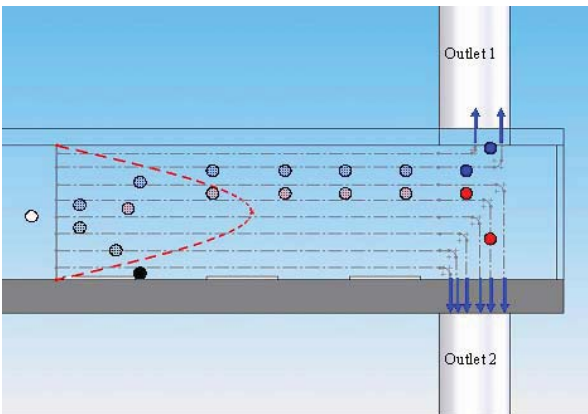

Fig. 16. Equal flow rates for outlet 1 and 2.

Fig. 17. Different flow rates for outlet 1 and 2.

4   Conclusion

In this paper, a numerical study was presented to investigate separation and trapping of particles using both negative and positive DEP based on an interdigitated microfludic device. The effects of particle size, voltage, and initial height on the particle separation and trapping were addressed. For negative DEP, the levitation height is independent of particle size but the time to reach the levitation position decreases significantly with increasing particle size. The initial height plays an important role in separating particles. The higher the initial height, the quicker the particle reaches the levitation position. For positive DEP, the effects of the particle size, initial height and voltage on the stopping distances were discussed. The bigger the particle size, the smaller the stopping distance; the higher the initial height, the longer time to be trapped; the

higher the voltage, the quicker to trap the particles. These simulation results are expected to be helpful to optimize microdevices.

References:
[1] M.P. Hughes, Strategies for dielectrophoretic separation in laboratory-in-a-chip systems, *Electrophoresis*, 23, 2002, pp. 2569-82.
[2] H.A. Pohl, *Dielectrophoresis*, Cambridge: Cambridge University Press, 1978.
[3] H.B. Li, R. Bashir, Dielectrophoretic separation and manipulation of live and heat-treated cells of Listeria onmicrofabricated devices with interdigitated electrodes, *Sensor Actuat. B – Chem.* **86**, 2002, pp. 215-21.
[4] Y. Huang, X.B. Wang, F.F. Becker, P.R.C. Gascoyne, Introducing dielectrophoresis as a new force field-flow fractionation, *Biophys. J.*, 73, 1997, pp. 1118-29.
[5] Y. Huang, R. Pethig, Electrode design for negative dielectrophoresis, *Meas. Sci. Technol.*, 2, 1991, pp. 1142-6.
[6] H. Morgan, M.P. Hughes, N.G. Green, Separationof submicron bioparticles by dielectrophoresis, *Biophys. J.*, 77, 1999, pp. 516-25.
[7] T. Schnelle, T. Muller, C. Reichle, G. Fuhr, Combined dielectrophoretic field cages and laser tweezers for electrotation, *Appl. Phys. B*, 70, 2000, pp. 267-74.
[8] D.F. Chen, H. Du, W.H. Li, C. Shu, Numerical Modeling of Dielectrophoresis Using a Meshless Approach, *Journal of Micromechanics and Microengineering*, 15 (5), 2005, pp. 1040-1048.
[9] A.J. Goldman, R.G. Cox, H. Brenner, Chemical Engineering Science 22, 1997, pp. 653-660.
[2] T.B. Jones, *Electromechanics of Particles*, New York: Cambridge University Press, 1995.